Optical and Quantum Electronics **23** *(1991) S267–S286*

Tunable far-infrared solid-state lasers based on hot holes in germanium

E. GORNIK
Walter-Schottky-Institut, TU-München, D-8046 Garching, FRG

K. UNTERRAINER, C. KREMSER
Institut für Experimentalphysik, Universität Innsbruck, A-6020 Innsbruck, Austria

Received 10 January 1990

The basic principles for achieving population inversion and stimulated emission in the far-infrared from *p*-Ge are discussed. In the heavy–light hole lasing mode a broad gain region is found resulting in a broad multimode spectrum due to intracavity modes. By attaching external plates of germanium a single mode operation is realized. The obtained powers are in the W range with linewidths of $\approx 0.2\,cm^{-1}$. A single mode magnetically tunable coherent source is achieved with the light hole cyclotron resonance laser. With external mirrors a tuning range from 20 to $120\,cm^{-1}$ with magnetic fields between 1 and 6 T is achieved. The intensity of the single mode is in the order of W, the linewidth below $0.2\,cm^{-1}$.

1. Introduction

It is a rather old idea to use the population inversion of hot carriers in bulk semiconductors to generate coherent sub-mm and mm radiation. The first proposal came in 1958 from Krömer [1] who suggested a negative mass amplifier (NEMAG). A concept for a magnetically tunable laser based on radiative transitions between Landau levels was proposed in the early 1960's by Lax [2] and Wolff [3]. Lax has suggested a cyclotron maser in *n*-InSb pointing out that the non-parabolicity causes unequally spaced Landau levels. Wolff proposed in addition that a sudden decrease in relaxation time above a certain energy level terminates the Landau ladder; thereby effectively eliminating upward transitions by electrons excited into higher levels. Nearly a decade later spontaneous cyclotron emission in a semiconductor was observed for the first time by Gornik [4] in 1972 and by Otsuka's group [5] in 1973.

It is quite remarkable that it took another decade of intense investigations of hot carrier phenomena until a solid-state laser in the far-infrared (FIR) spectral region could be realized: a cyclotron resonance (CR) laser based on light hole transitions in *p*-Ge was first demonstrated by Ivanov and Vasil'ev [6] in 1983, the light–heavy hole laser in *p*-Ge by Andronov *et al.* [7] in 1984.

This success would not have been possible without the intense theoretical study of highly anisotropic carrier distribution functions resulting from optical phonon emission by several groups [8–17]. It was the pioneering work of Vosilyus and Levinson [9, 10] and by

0306-8919/91 $03.00 + .12

Kurosawa and Maeda [11, 12] which found inverted carrier distributions in the case of streaming for crossed electric and magnetic fields. In the following it was the Russian theoretical work around Andronov and Pozhela [18] which tried to obtain a bulk high frequency negative differential resistivity which would provide an active medium for the realization of the CR maser. The basic idea was that a scattering-free transit of carriers up to the energy of the strong scattering threshold (optical phonon emission) can provide not only an inverted hot carrier distribution but also a mechanism for a dynamic negative differential resistance (for reviews see [19] and [20]).

The first report on stimulated cyclotron resonance emission in the frequency range $40\,\mathrm{cm}^{-1} < \nu < 50\,\mathrm{cm}^{-1}$ from light holes in germanium came from Vasil'ev and Ivanov [6]. Electric fields between $1\,\mathrm{kV\,cm}^{-1}$ and $1.5\,\mathrm{kV\,cm}^{-1}$ and orthogonal magnetic fields between 1.5 T and 2.2 T were applied. Stimulated CR emission was also observed at higher magnetic fields with frequencies in the range $65\,\mathrm{cm}^{-1} < \nu < 85\,\mathrm{cm}^{-1}$ by Mityagin *et al.* [21]. The power of this emission was three orders of magnitude smaller than that of the light to heavy hole transitions [22]. The transitions involved have not yet been identified.

2. Pumping mechanisms

In high purity semiconductors, at low temperatures, carriers are strongly scattered when accelerated in external fields up to the optical phonon energy. They gain energy practically collisionless from the field. If we consider a *p*-type semiconductor with a light and heavy hole mass m_l and m_h respectively, the conditions for streaming are met at different electric (E) and magnetic (B) fields. The situation is best described in a schematic representation of hole trajectories in the $v_z = 0$ plane in crossed $\boldsymbol{E}$ and $\boldsymbol{B}$ fields. The centre P of the cyclotron orbits is $(0, -E/B)$. In Fig. 1a the situation when the heavy holes are streaming and the light holes are accumulated is sketched. For a given E/B ratio the centre P is the same for both types of carriers. However, the velocity corresponding to the optical phonon energy ($\hbar\omega_{op}$) is quite different: $v_{op}^{l,h} = (2\hbar\omega_{op}/m_{l,h}^*)^{1/2}$ since it depends on the effective mass (m*). From Fig. 1a it is evident that several Landau levels lie within the optical phonon energy for light holes, which leads to an accumulation of light holes in a limited area of velocity space. The heavy holes are streaming: they are accelerated collisionless to the optical phonon energy and scattered back to the origin. The resulting distribution function is schematically shown in Fig. 1b. As a result of the accumulation the light hole distribution is inverted while the heavy holes are distributed nearly homogeneously up to the phonon energy.

The situation is best described by a dimensionless parameter $\xi_{h,l} = v_{op}^{h,l}/(E/B)$ which is the ratio between v_{op} and the orbit centre velocity E/B. The most efficient pumping process for light hole inversion is present when $1 < \xi_h < 2$ and $\xi_l > 2$. According to a classical calculation for *p*-Ge by Andronov *et al.* [20] with $m_h^* = 0.35\,m_0$, $m_l^* = 0.043\,m_0$ and $\hbar\omega_{op} = 37\,\mathrm{meV}$, the optimum condition of the ratio E/B for stimulated emission is $\xi_h \approx 1.4$ and $\xi_l = 2.85$. In this case stimulated emission covers the emission range $\lambda = 40$ to $400\,\mu\mathrm{m}$, where the λ-position for the maximum gain shifts to lower values (higher energy) with increasing B (or E).

In terms of a laser pumping process we can sketch a four level pumping scheme which illustrates the process quite well (Fig. 2a). The streaming process is represented by the ground level at $v_h \approx 0$ and the upper level at $v_h = v_{op}^h$. Scattering transfers heavy holes either directly into the light hole accumulation region or by an emission of one optical

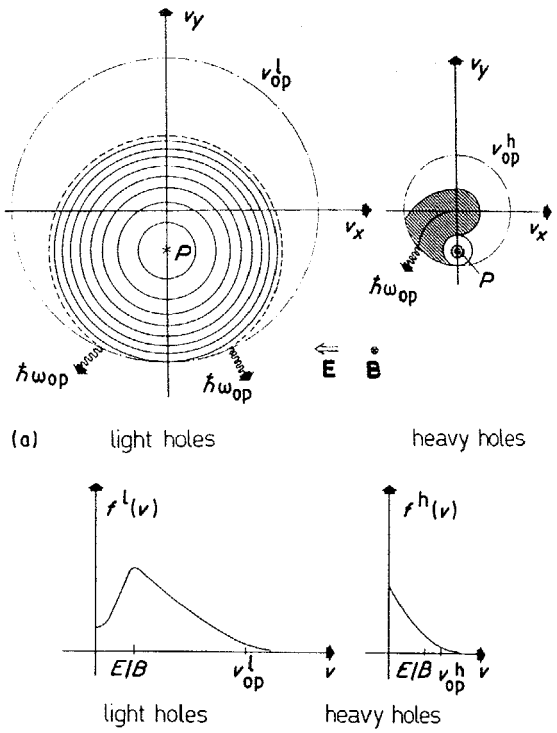

Figure 1 Schematic representation of (a) hole trajectories in the $v_z = 0$ plane for a crossed field configuration ($B = 1$T, $E = 1.4\,\mathrm{kV\,cm^{-1}}$) simulating a situation $\xi_l > 2$ and $\xi_h \approx 1.4$. The orbits for light holes correspond to Landau level, the shaded area for heavy holes to the streaming region; (b) light and heavy hole distribution function for the situation in (a).

phonon to $v_h = 0$: after consecutive tunnelling to the light hole band the carriers are accelerated to the accumulation region by the electric field. After radiative transitions light hole → heavy hole, the heavy holes are transferred by the electric field back to the streaming process. In Fig. 2b the same four step process is shown within the valence band bandstructure for clarity indicating the same transitions. Detailed calculations of the gain coefficient under the above situation have been performed by Pozhela *et al.* [23, 24] already before the observation of stimulated emission.

An inversion between Landau levels in a crossed field situation was first predicted by Al'ber *et al.* [25] and Kurosawa [14]. In Fig. 3 a situation for $\xi \geqslant 2$ is shown in the velocity space as predicted in [14]. The cyclotron orbit (Landau level $n = 3$) through $|v| = 0$ is called the main trajectory and is not disturbed by the optical phonons. Carriers in higher Landau levels interact strongly with optical phonons resulting in a small velocity after the phonon emission. Therefore the population of the main trajectory (Landau level $n = 3$) is increased and an inversion occurs between the $n = 3$ Landau level and lower Landau levels, which are not influenced by carriers scattered by optical phonons. This inversion corresponds to a torus type distribution function in the velocity space.

Helm *et al.* [26, 27] employed a fully quantum mechanical treatment for the light holes in *p*-Ge considering optical and acoustic deformation potential scattering. Kozlov *et al.* [28] showed in a Monte-Carlo simulation that impurity scattering enhances an inversion due

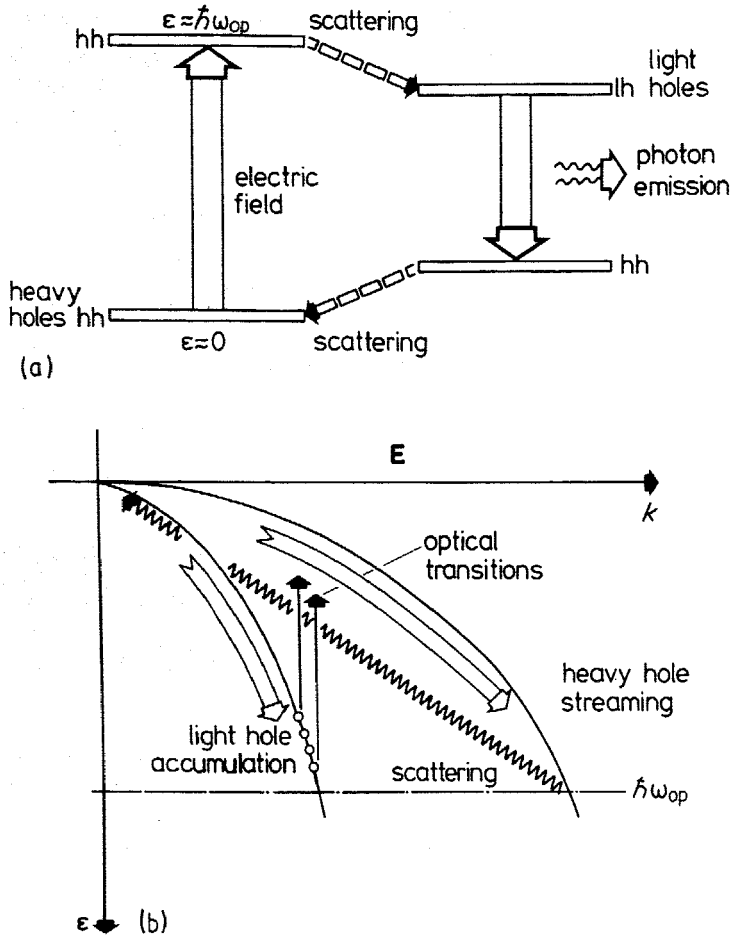

Figure 2 (a) Schematic four level pumping scheme for the heavy–light hole laser process. (b) Band structure of *p*-Ge. The different pumping, scattering and optical transitions are indicated for the lasing process.

to the decrease of the impurity scattering rate with increasing energy of the carriers. D'yakonov and Perel' [29] suggested a semi-classical model of tunnelling transitions between the Landau levels of heavy holes and light holes. The tunnelling probability is high for low-lying light hole Landau levels; therefore the lifetime of the carriers in the low Landau levels is shorter than in the high levels and a population inversion can be built up.

Gorbovitskii [30] showed that the Landau levels of heavy holes and light holes are strongly mixed due to a strong coupling between the two bands. As a consequence the lifetime of light hole Landau levels is influenced by the lifetime of heavy holes. For certain values of the external fields where mixing takes place the lifetime of low lying light hole Landau Levels is reduced since the heavy holes are in streaming motion which results in a short lifetime.

Thus, the basic pumping mechanism for a Landau level inversion of the light holes is streaming motion of the heavy holes and mixing or tunnelling between the levels at low energies.

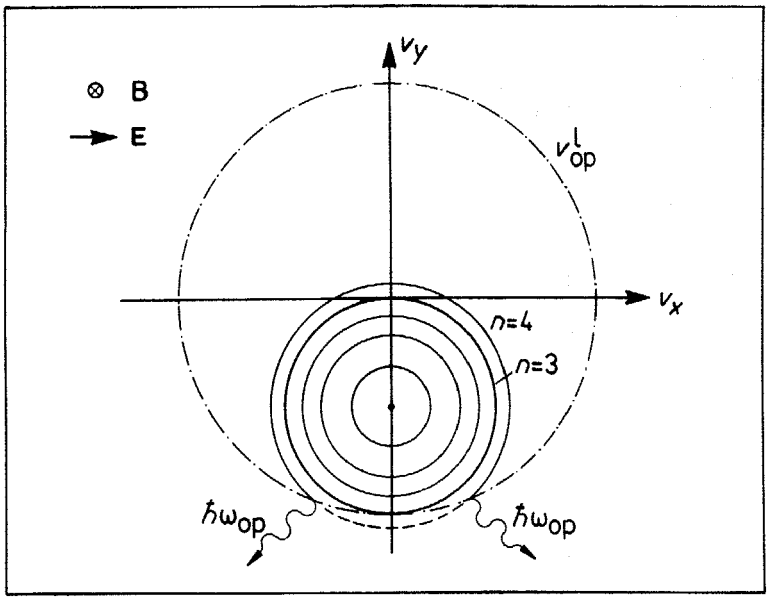

Figure 3 Cyclotron orbits of several Landau levels in velocity space in crossed electric and magnetic field (E = 2.7 kV cm^{-1}, B = 1 T). The (–·–·–·–) circle corresponds to the critical velocity v_{op}.

3. Light hole–heavy hole laser oscillation

Experimental studies started with the observation of spontaneous emission in p-Ge [30–33] in 1981/82 and were followed only few years later by the first success in observing stimulated emission by the Russian group around Andronov [7] and the subsequent observation by Komiyama *et al.* [35] and Helm *et al.* [36].

In this chapter a study of the stimulated emission from p-Ge in the light–heavy hole mode is presented. By investigating samples with different dimensions with a broadband (p-Ge) and narrowband (n-GaAs) detector the intensity, the spectrum and the mode behaviour is obtained.

Three different samples were used for the experiments, all cut from a Ga-doped Ge-crystal with $p = N_A - N_D = 1.2 \times 10^{14}$ cm^{-3}. The sample dimensions are given in Table I.

The distance between the electrical contacts is d, l is the sample length in the direction of the magnetic field (in our case the [111] direction), and a is the width. Electrical contacts were made by evaporating indium (with some gold) and alloying at 400°C. All faces of the samples were polished and are parallel within 30″, which turned out to be crucial for the achievement of laser oscillation. Voltage pulses of up to 1000 V with 1 μs duration were applied to the samples with a low impedance high power pulse generator. The typical current through the samples was 200 A, in accordance with the relation $j = 1/2 pev_{op}^h$,

TABLE I Sample dimensions

Sample	d	a	l (mm)
1	3.7	2.4	46.9
2	4.2	3.15	43.1
3	5.2	3.75	48.4

where j is the current density, and $1/2\, v_{op}^{h}$ is the approximate drift velocity of the heavy holes under 'streaming motion' conditions [37]. The pulse repetition rate was chosen to be around 5 Hz. For rates higher than 10 Hz lasing breaks down due to the sample heating. The experiments were performed at 4.2 K, so the sample was immersed in liquid helium at the centre of a superconducting solenoid. To check the range of electric and magnetic fields where lasing can be achieved, the radiation was detected with a broadband Ge:Ga-detector with peak sensitivity at about 110 μm. A magnetic field tunable narrow-band GaAs-detector was used for the detailed analysis of the emission spectrum. It was placed in the centre of a second magnet in the cryostat below the sample. The Zeeman-split $1s$-$2p^{+}$ shallow donor line is used for detection [38]. This line is tubable between 45 and 130 cm^{-1} for magnetic fields of 1 to 6.5 T. Due to the fact that the GaAs contains only one chemical species of shallow donor, the absorption line is extremely narrow (0.25 cm^{-1}), and the GaAs can be used as a high resolution spectrometer.

Fig. 4 shows typical traces of stimulated emission from sample 2, recorded with a Ge:Ga-detector. The detector signal due to stimulated emission is a factor of 10^2 to 10^3 above the level of spontaneous emission. The region of lasing extends from somewhat less than $B = 1$ T for the lowest electric field of $E \approx 1000\ V\,cm^{-1}$ up to 2 T for $E \approx 2000\ V\,cm^{-1}$. This corresponds to $1.1 < \xi_h < 1.7$. These data agree quite well with the results of other authors [7, 20, 35, 39–41]. Comparing the magnitude of the signal with the signal obtained

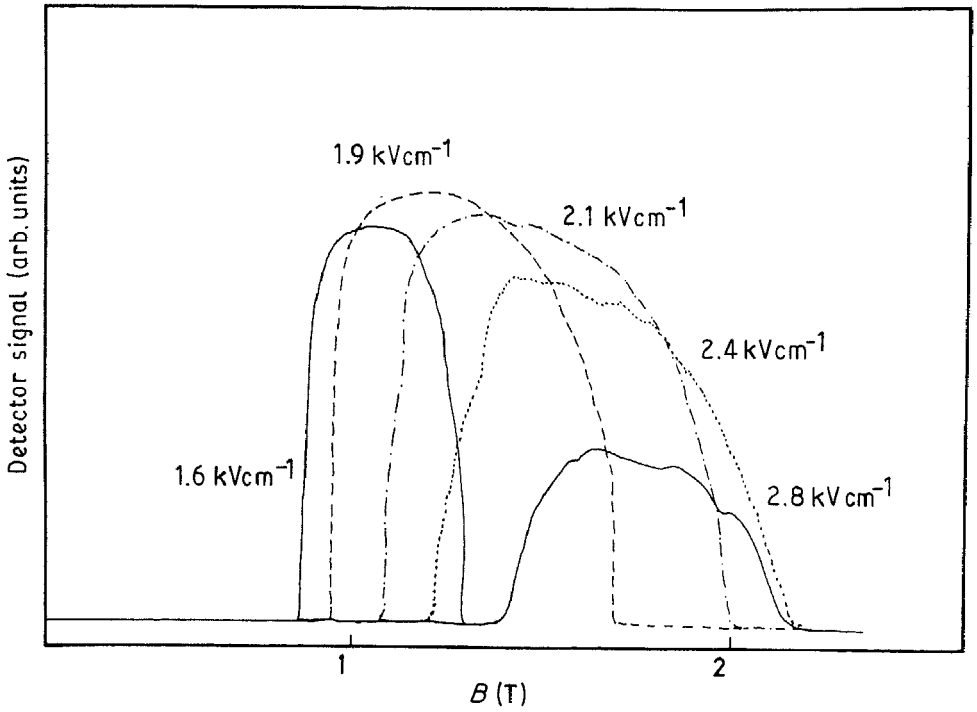

Figure 4 Ge:Ga-detector signal from sample 2 as a function of magnetic field for different electric field values.

from a (far-infrared) FIR gas laser and an InSb-Landau source, the emitted power was estimated to reach 500 mW.

To analyse the spectrum of the stimulated emission the electric and magnetic fields applied to the sample were set to a fixed value, while the magnetic field of the GaAs-detector was tuned. Using the $1s$–$2p^+$ shallow donor transition, the frequency of the detected radiation is linearly related to the magnetic field over a wide range. Fig. 5 shows three spectra from sample 2, for three different values of the electric and magnetic field. The spectra consist of 10 to 20 lines with a regular mode spacing of about $1.4\,cm^{-1}$. Their positions remain fixed with changes in the applied fields. In the high-gain region some additional lines appear, disturbing the regular structure. The measured widths are about $0.4\,cm^{-1}$. We conclude that the real linewidth of the emission is of the same order of magnitude as the detector linewidth ($0.25\,cm^{-1}$). By varying the electric and magnetic fields it is possible to obtain lasing between 75 and 110 μm. There is a general trend towards emission at shorter wavelengths for both higher E- and B-fields (see Fig. 5).

Andronov *et al.* [7] and Komiyama *et al.* [35] suggested that the lasing modes are due to total reflections at the sample surfaces, since without mirrors the quality factor of the cavity is far too low to allow longitudinal or transverse modes to oscillate (the Ge surface has 36% reflectivity at normal incidence). According to Fig. 6 the observed mode spacings are 1.74 and $1.20\,cm^{-1}$ for samples 1 and 3, respectively, and $1.40\,cm^{-1}$ for sample 2 (not shown). Comparing the spacings with the dimensions of the samples it appears to be very likely that the width, a, is the crucial parameter determining the mode spacing (see Table I).

The mode spacings can be explained by considering the transverse resonance condition given by $k_x n = kn \sin\theta = M\pi/a$, where n is the refractive index, M is an integer, and θ is the angle between k and the longitudinal axis of the crystal (see insert in Fig. 6). The

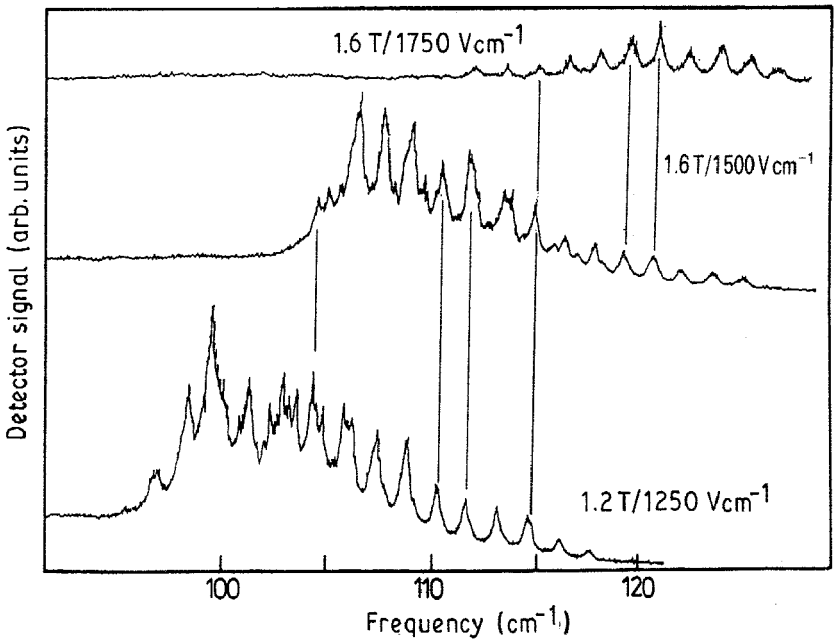

Figure 5 Spectrum of stimulated emission from sample 2 for different electric and magnetic fields.

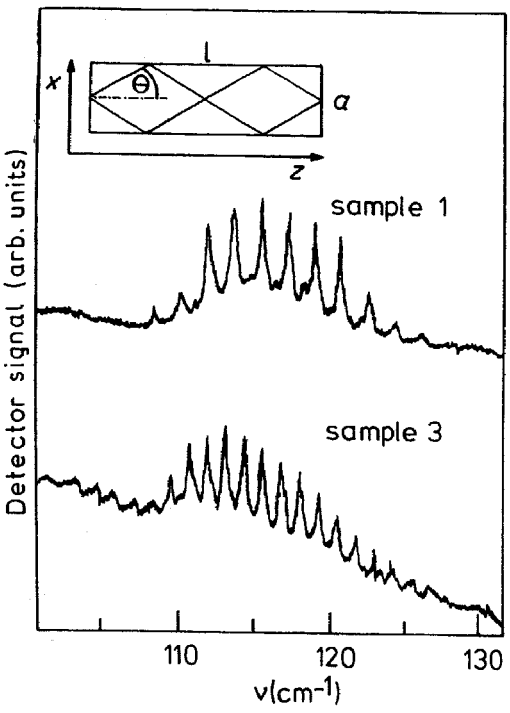

Figure 6 Spectrum of stimulated emission for different electric and magnetic fields. Sample 1: $E = 1.8\,\mathrm{kV\,cm^{-1}}$, $B = 1.4\,\mathrm{T}$. Sample 3: $E = 1.9\,\mathrm{kV\,cm^{-1}}$, $B = 1.7\,\mathrm{T}$. The insert schematically shows the ray path in the germanium crystal.

analogous longitudinal resonance condition is not considered, because it would yield a very narrow mode structure which is not observed in the experiment. In addition, we have the geometrical condition $\tan\theta = Na/l$ (N is an integer), which ensures that the path of the ray is closed within the sample. This leads to a mode spacing (in wave numbers) $\Delta\nu = (2an\sin\theta)^{-1}$. θ must satisfy the condition $14.5° < \theta < 75.5°$, because 14.5° is the angle of total reflection for germanium. One can assume that modes with the smallest possible θ have the lowest losses, because they undergo the fewest reflections. Thus, for each sample the mode spacing is determined first by choosing the angle θ with the smallest possible N, and then this angle is used in the expression for $\Delta\nu$. This procedure gives a mode spacing $\Delta\nu$ of $1.77\,\mathrm{cm^{-1}}$ ($N = 6$), $1.41\,\mathrm{cm^{-1}}$ ($N = 5$), and $1.14\,\mathrm{cm^{-1}}$ ($N = 4$), for samples 1, 2 and 3, respectively, in good agreement with the measured values. This interpretation is confirmed by the work of Andronov *et al.* [41], who reported emission of a single line by using a very thin ($a = 0.7\,\mathrm{mm}$) sample, where the mode spaching is as wide as the gain region.

After attaching external mirrors to sample 3 (see insert in Fig. 7), the region of electric and magnetic fields where lasing occurs stays roughly the same. The detector signal is also of the same order of magnitude with and without mirrors. The observed spectra, however, exhibit a dramatic change. Fig. 7 shows spectra of sample 3 for different electric and magnetic fields, recorded with the GaAs detector. A considerably reduced number of lines appear with wider mode spacing and higher amplitude, accompanied by some other less dominant structure. Varying the electric and magnetic fields allows us to switch on and off lines on the long or short wavelength side of the spectrum due to a change in the gain spectrum. In this way it was possible to obtain operation of a single line (lower part of Fig. 7). The emission wavelength is $87.3\,\mu\mathrm{m}$ ($114.5\,\mathrm{cm^{-1}}$), the adjacent line at $83.3\,\mu\mathrm{m}$ ($120.0\,\mathrm{cm^{-1}}$) is just at threshold. As is seen from Fig. 7 the single line contains approximately

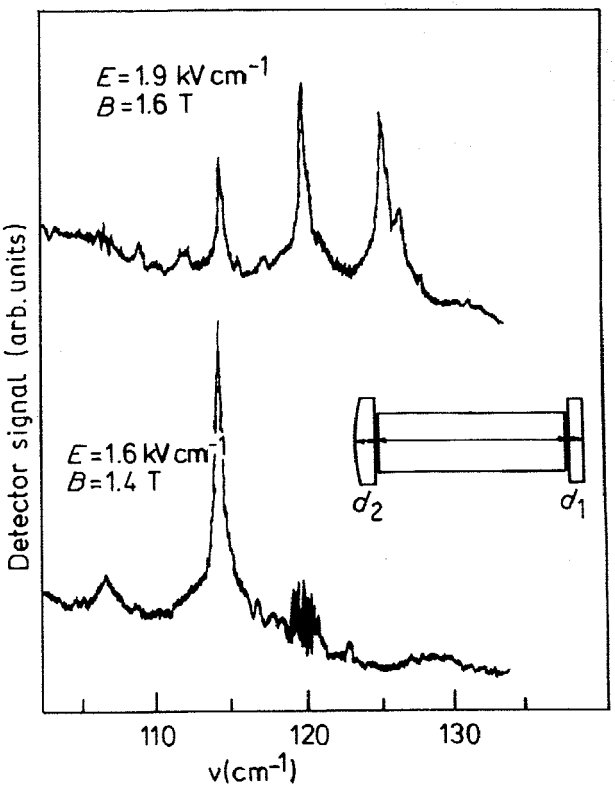

Figure 7 Emission spectra from sample 3 after attaching external mirrors for different electric and magnetic fields. The insert shows the cavity configuration.

the same total intensity as the three lines together. However, one cannot exclude the coexistence of several cavity modes within this line, because their spacing would be below the resolution of the detector. The spectra observed by Andronov *et al.* [41] from samples with external mirrors showed a very irregular and complicated structure. Komiyama and Kuroda [39] reported some changes in the spectrum and were able to reduce the number of oscillating lines by sandwiching a thin layer of TPX between the sample and one mirror.

The mode spacing in Fig. 7 is equal to $\Delta\nu = 5.5\,\mathrm{cm}^{-1}$, which is too large for fundamental longitudinal or transverse cavity modes. A possible explanation is the formation of an intracavity interference filter by the two Ge-plates: since they are not subject to the electric field like the sample, they have a slightly different index of refraction [41]. Also the thin layer between sample and mirror induces a change of the refractive index, which provides the possibility of Fabry–Perot like reflections. A thickness of $d_1 = 0.9\,\mathrm{mm}$ and $d_2 = 1.1\,\mathrm{mm}$ (the slight curvature of the convex plate is neglected) would give a spacing of only $1.4\,\mathrm{cm}^{-1}$ and $1.1\,\mathrm{cm}^{-1}$, respectively. If, however, the combined resonance condition for both plates is considered, one gets spacings between 4 and $6\,\mathrm{cm}^{-1}$ for a low finesse of the Fabry–Perots.

To ensure that for a wide range of the external fields only one line is oscillating, the geometrical mode spacing of the resonator has to be larger than the gain region (7 to $8\,\mathrm{cm}^{-1}$). By inserting a silicon spacer with a thickness of $30\,\mu\mathrm{m}$ between sample and mirror

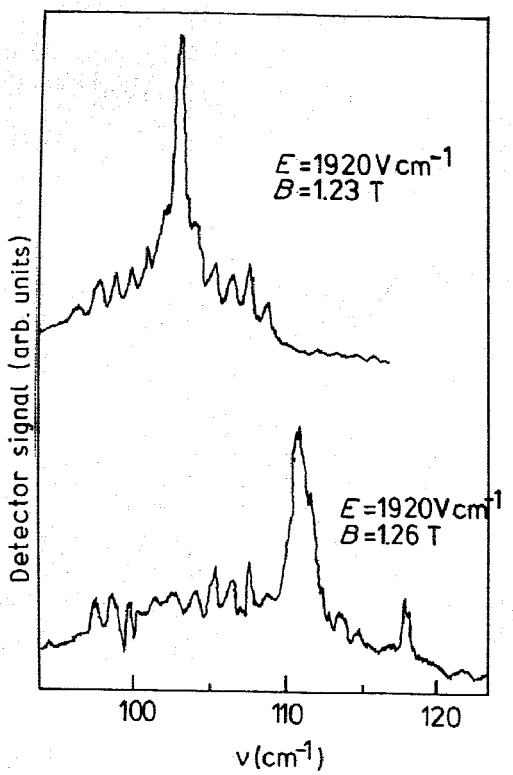

Figure 8 Spectra of the sample with a 30 μm silicon spacer inserted between the sample and flat germanium mirror in the configuration shown in Fig. 7.

it is possible to obtain single mode operation in almost the complete range of external fields where lasing occurs without mirror (Fig. 8) [43]. This line can be tuned to shorter wavelengths with higher external fields by shifting the gain region. The mode spacing is about 9 cm^{-1}. In addition several weak lines occur with a mode spacing of about 1.1 cm^{-1}. The silicon spacer cannot act as an interference filter as the reflectivity on both interfaces is determined only by the small difference of the refractive index between silicon ($n = 3.5$) and germanium ($n = 4$). In the case of the germanium mirrors the reflectivity is high on one side due to the metallic coating. However, the silicon slab enlarges the discontinuity of the refractive index between the sample and the plane mirror and therefore the finesse of this mirror is increased. Thus its Fabry–Perot resonances become sharper in comparison to that of the curved mirror. This is evident through the appearance of the weak lines in Fig. 8 with a mode spacing of 1.1 cm^{-1}, which are due to Fabry–Perot resonances within the plane mirror. The most important effect is that the combined Fabry–Perots resonance is increased (9 cm^{-1} according to Fig. 8). As a consequence only one single line is oscillating within the gain region.

Tuning is possible now by changing the gain region: the gain region can be shifted by the external field between 90 cm^{-1} and 130 cm^{-1}. When the gain region is shifted by more than the geometrical mode spacing to shorter wavelengths an according mode with a shorter wavelength starts up, because it is now lying inside the gain region. The previous mode is now outside the gain region and cannot oscillate anymore. Therefore we can tune the single line in steps of geometrical mode spacing of the resonator (in our case 9 cm^{-1}) between 90 cm^{-1} and 130 cm^{-1} by changing the external fields.

The polarization characteristics and the effects of uniaxial stress on the laser oscillations were studied by Komiyama [40]. The gain of the laser is found to be rather small in the range of 5×10^{-3} to $10^{-2}\,\mathrm{cm}^{-1}$ which explains the necessary high quality factor of the cavity.

4. Light hole cyclotron resonance laser

The most important achievement in the field was the discovery of stimulated Landau emission from light holes by Ivanov and Vasil'ev [6]. During the investigation of spontaneous emission in crossed fields in an extremely pure germanium sample ($p = 8 \times 10^{12}\,\mathrm{cm}^{-3}$) an intensity spike was detected in the sensitivity region of the GaAs detector. Further investigation of this radiation, including the analysis of the spectrum with external mirrors resulted in laser radiation in the wavelength range between 210 and 350 μm [44, 45]. A considerably lower power than in the light hole – heavy hole mode of about 1 mW was found. The frequency of the radiation corresponds to the cyclotron frequency of holes with a mass of $m_l^* = 0.0464\,m_0$. The linewidth of emission was below $0.5\,\mathrm{cm}^{-1}$. In the following also Mityagin *et al.* [21, 46] observed stimulated Landau emission from light holes in *p*-Ge. The first demonstration of this lasing effect outside Russia was achieved by Unterrainer *et al.* [47]. The first single line tunable far infrared laser was demonstrated with samples of 4 to 6 cm length when external resonators were applied [21, 47]. The resonators consist of two copper mirrors (isolated by mylar foils), which were attached to the end faces. The light is coupled out by a 1 mm hole in one of the mirrors. The spectra obtained consist of a single laser line which can be tuned linearly by the magnetic field. The tuning characteristics for materials with a doping below $10^{13}\,\mathrm{cm}^{-3}$ is well described by the relation

$$\omega_c(\mathrm{cm}^{-1}) = eB/m_l^* = 20.1\,B(\mathrm{T})$$

with m_l^* the light hole mass. For a doping of $8 \times 10^{12}\,\mathrm{cm}^{-3}$, lasing is observed between 30 and $50\,\mathrm{cm}^{-1}$ [45]. The power levels reported were in the range of a few mW.

To understand the pumping mechanism in the cyclotron mode the orientation dependence of **E** and **B** in respect to the crystallographic axis was investigated by different groups: Vasil'ev and Ivanov [44] have found that only two pairs of $\mathbf{E} \perp \mathbf{B}$ orientation $\mathbf{B} \parallel [1\bar{1}0]$, $\mathbf{E} \parallel [112]$ and $\mathbf{B} \parallel [111]$, $\mathbf{E} \parallel [11\bar{2}]$ provide population inversion by streaming pumping, while in the $\mathbf{B} \parallel [100]$, $\mathbf{E} \parallel [001]$ orientation no inversion is expected. A similar result was reported recently by Mityagin *et al.* [21], who found the magnetic field orientation $\mathbf{B} \parallel [111]$ most favourable. The details of the pumping mechanism and the induced stimulated transitions have not been identified so far.

A breakthrough was obtained by Unterrainer *et al.* [47] with the orientation $\mathbf{B} \parallel [110]$ and $\mathbf{E} \parallel [1\bar{1}0]$. Whereas in previous work intensities in the order of several mW were reported, intensities comparable to the lh–hh mode are found in this configuration for a sample doping of $6 \times 10^{13}\,\mathrm{cm}^{-3}$.

In this paper we report on the study of strong narrowband stimulated CR emission in the frequency range between $65\,\mathrm{cm}^{-1}$ and $85\,\mathrm{cm}^{-1}$ due to Landau level inversion within the light hole sub-band of germanium. The emission power is comparable to the stimulated light to heavy hole emission. Using different output couplers we have determined the gain to be $0.05 \pm 0.02\,\mathrm{cm}^{-1}$. We have studied the spectrum of the stimulated emission by means of an extremely narrowband, magnetic field tunable *n*-GaAs detector. The emission spectrum consists of a single line which is linearly tunable with magnetic field. For the first time we have identified the Landau levels involved in the lasing process.

For the experiments, samples with a carrier concentration of $N_A - N_D = 6 \times 10^{13}\,cm^{-3}$ were used. The length of the samples parallel to the [110] crystallographic direction was between 20 and 40 mm. The side faces were parallel to the $[1\bar{1}0]$ and to the [001] directions, respectively. The section was typically $5 \times 5\,mm^2$. All faces of the samples were polished and were parallel within 30″. The magnetic field was applied parallel to the [110] direction and the electric field parallel to the $[1\bar{1}0]$ direction. Electrical contacts were made by evaporating indium (with 5% gold) or aluminium and alloying at 400°C. To form an external resonator, two copper mirrors were fixed to the endfaces of the sample with a thin insulating layer between the sample and the metal mirrors. Mirrors with different bores between 0.7 and 1.5 mm were used as output couplers. The experiments were performed at 4.2 K, so the sample was immersed in liquid helium at the centre of a superconducting solenoid. Voltage pulses of up to 2000 V with 1 μs duration were applied to the sample with a high power low impedance pulse generator.

Fig. 9 shows the emission signal of sample 1 as a function of the applied magnetic field recorded with a broadband Ge : Ga detector. The detector signal due to stimulated emission is 2 to 3 orders higher than that from the spontaneous emission. Lasing was observed for two different ranges of the magnetic field. The lower range ($1 < B(T) < 2$) is due to light to heavy hole transitions. The spectrum of this emission is broadband [35, 36]. The higher field range ($3 < B(T) < 4$) corresponds to *stimulated cyclotron resonance* emission.

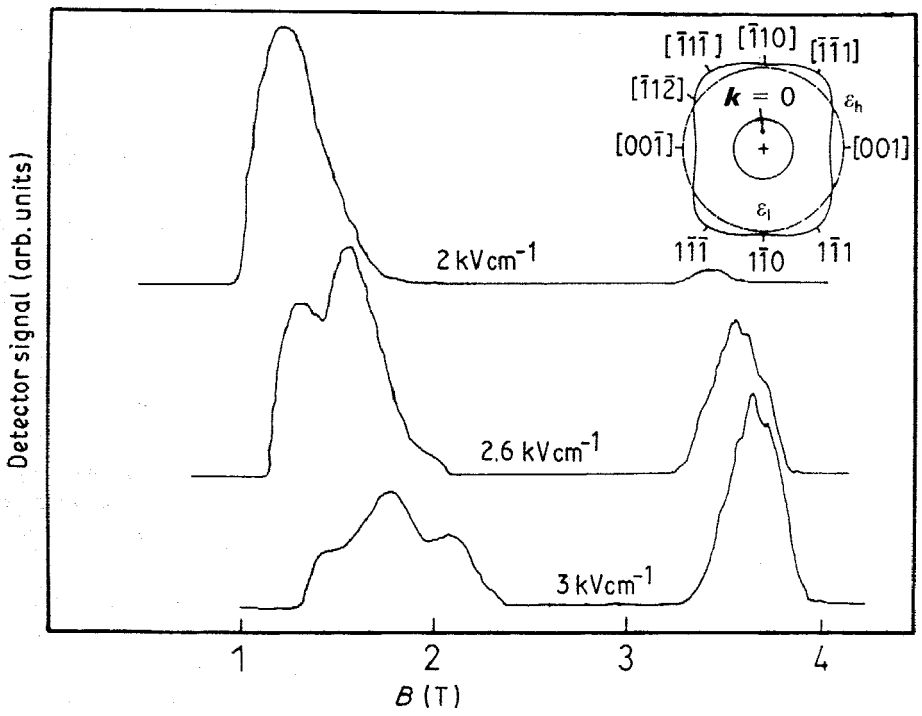

Figure 9 Stimulated FIR emission as a function of the magnetic field for different electric fields, recorded with the Ge : Ga detector. At lower magnetic fields the emission signal is due to stimulated light to heavy hole transitions; at higher fields the signal is due to the stimulated CR emission of the light holes. The inset shows the lines of constant energy for heavy and light holes.

For higher electric fields the intensity of the stimulated CR emission increases while the intensity of the emission from light to heavy hole transitions diminishes. The power of the stimulated CR emission is of the same order of magnitude as that of the interband emission which was estimated earlier by comparison with a FIR gas laser to be about 500 mW. Stimulated CR emission is observed for magnetic fields between 3 and 4.2 T and electric fields between 1.5 and 3.6 $kV\,cm^{-1}$.

In Fig. 10 the emission is shown as a function of the magnetic field detected with the Ge:Ga-detector for sample 1 with external mirrors (dashed curve) and for comparison without external mirrors (solid curve). Without external resonator the emission power fluctuates by about 40% within the tuning range due to the occurrence of waveguide-like modes caused by internal reflection at the sample surfaces [35, 36]. The output power with the external resonator is a factor of 40 larger than without the resonator and the fluctuations are only 20%. In this resonator configuration longitudinal modes are able to oscillate. Since these modes do not undergo total reflections at the sample endfaces, more power is coupled out by the hole of the mirror and the necessary gain for threshold is increased. Thus the range of the stimulated emission is smaller than without the resonator. By controlling the output power with mirrors with different holes and therefore different transmission we calculate the gain to be $0.05 \pm 0.02\,cm^{-1}$.

For a detailed analysis of the stimulated CR emission a magnetic field tunable, high resolution ($\Delta\nu = 0.25\,cm^{-1}$) GaAs detector was used. Fig. 11 shows spectra (intensity versus frequency) from sample 1 for different electric and magnetic fields: each spectrum consists of a single line. The position of the line can be changed by varying the magnetic

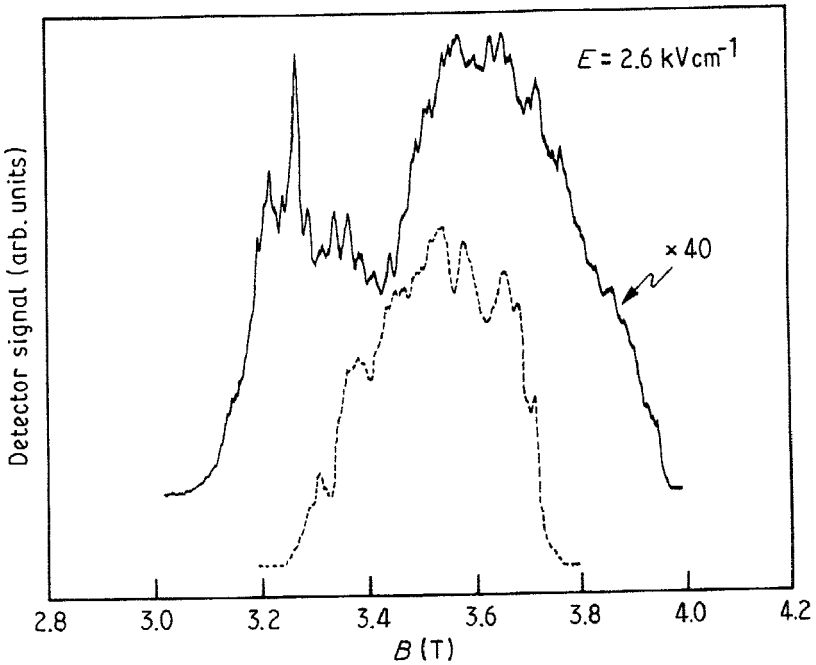

Figure 10 Stimulated CR emission of sample 1 without external resonator (——), and with external resonator (– – –) as a function of the sample magnetic field, detected by a Ge:Ga detector.

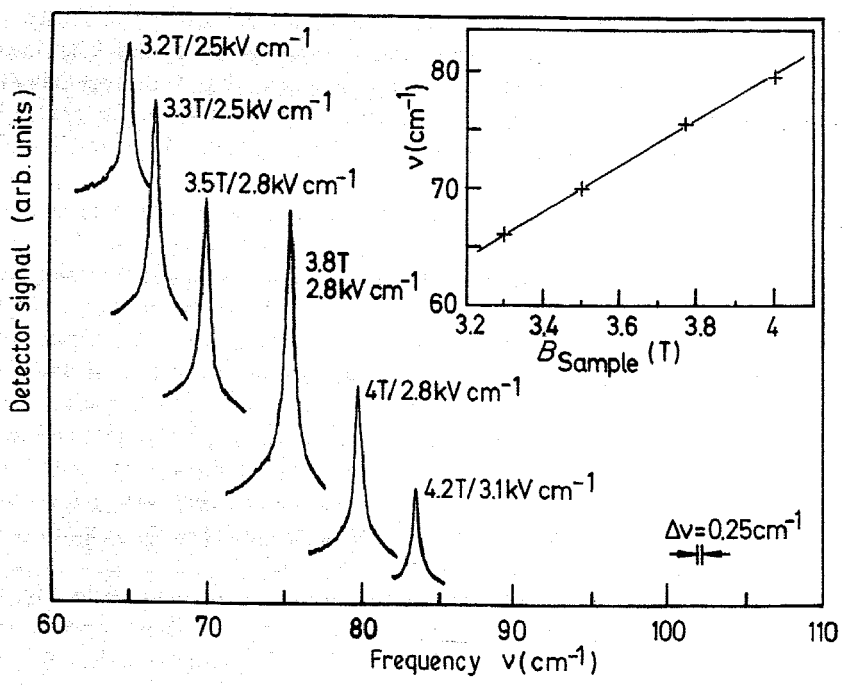

Figure 11 Spectra of the stimulated emission from sample 1, recorded by a GaAs detector. The spectra consist of a single line which is tunable with the magnetic field. The inset shows the frequency of the emission lines versus applied magnetic field.

field in a range between 65 cm^{-1} and 85 cm^{-1}. In the inset in Fig. 11 the frequency of the emission line is plotted against the applied magnetic field. The data points are all on one straight line and the emission frequency corresponds to the cyclotron resonance frequency of the light holes $\omega_c = eB/m_l^*$ where $m_l^* = 0.0466 \pm 0.001\, m_0$. The relation between frequency ω_c and magnetic field B is given by $\omega_c\,(\mathrm{cm}^{-1}) = 20.05B(\mathrm{T})$ which is a somewhat different value than that found by Vasil'ev and Ivanov [45]. The measured linewidth is about 0.45 cm^{-1}; by taking into account the resolution of the GaAs detector, we conclude that the real linewidth of the emission is about 0.2 cm^{-1}, which is significantly narrower than the spontaneous linewidth of about 3 cm^{-1}. We believe that the linewidth in our case is determined by the fact that the magnetic field of the solenoid used is not homogeneous over the whole length of the sample.

In order to help with the identification of the lasing transition we performed a CR absorption measurement with sample 1 and compared the results to the emission data [48]. Fig. 12 shows the transmission of sample 1 obtained with the 75.12 cm^{-1} line of an external FIR gas laser as a function of the applied magnetic field, detected with the GaAs detector. When the carriers are heated by small electric fields (15 V cm^{-1}) a minimum occurs due to CR absorption of the light holes. The absorption line has a shoulder at the high magnetic field side. In the lower part of Fig. 12 the spectrum of the stimulated CR emission is recorded with the GaAs-detector set to 75.12 cm^{-1}. The maximum of the signal is at higher magnetic fields than the minimum of the absorption.

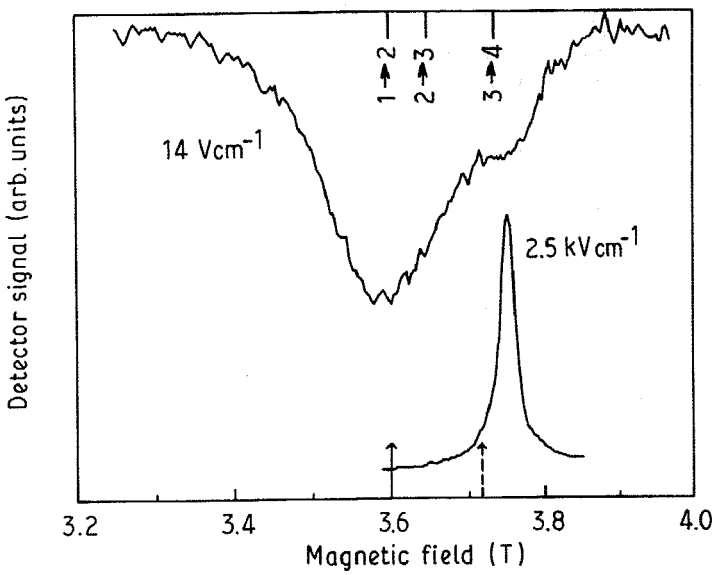

Figure 12 Transmission of the 75.12 cm^{-1} line of an external FIR gas laser in sample 1: at low electric field cyclotron resonance absorption occurs. In the lower part the spectrum of stimulated CR emission is shown, recorded with a GaAs detector set to 75.12 cm^{-1}. The vertical lines at the top represent the positions of the first three light hole transitions. At the bottom, (— — →) shows the n = 2 to 1 lasing transition shifted to higher effective mass due to the electric field. (——→) shows the position at zero electric field.

Because of the coupling between light and heavy hole bands, the light hole levels are not equidistant [49, 50]. The Landau level spacing may also be influenced by the electric field [21, 51]. In addition, the influence of the conduction and spin–orbit split-off bands are important at these fields and energies, giving a significant non-parabolicity correction to the relevant light hole energy levels (typically, of about 5% in the effective mass value). Thus, for a quantitative determination of the light hole transitions we used the Pidgeon and Brown (PB) model [52] which includes these effects, but has not previously been used by authors working in the hot hole laser field. Our method is to take the exact PB computation for germanium to give the *unperturbed* eigenvalues and eigenvectors for light and heavy hole Landau levels. We then go to the uncoupled (Luttinger) scheme to calculate the *shift* of these Landau levels in the electric field by second order perturbation theory [51, 54].

The PB computation for zero or very low electric field shows that the three 'lowest mass' ligh hole transitions that can occur in absorption are, in order: n = 1 to 2, n = 2 to 3, and n = 3 to 4 in the b-set (the a-set transitions have higher 'effective mass' and in any event, are not expected to support a population inversion [21, 30]). These transitions are indicated above the absorption spectrum in Fig. 12, and show very good agreement with the features observed. Evaluating the electric field shifts, we find that only the n = 1 to 2 transition is shifted significantly to higher magnetic field; at the experimental value of 2.5 kV cm^{-1} for the laser observation this agrees well with the measured position for laser emission, as indicated below the emission spectrum of Fig. 12 (in practice the effective internal electric field is higher due to the Hall field making the agreement with the experiment even better). The reason for this anomalous shift is that the n = 1 level is affected differently by the electric field from the higher n levels as a result of quantum effects referred

to above. At the field ranges where stimulated emission is observed the $n = 4$ level would be above the optical phonon frequency, making the $n = 3$ to 4 transition ineligible for population inversion; thus, the spectroscopy identifies the lasing transition to be $n = 2$ to $n = 1$ [48].

For the [110] direction the $n = 1$ Landau level of the light holes is strongly mixed with higher Landau levels of the heavy holes [21, 30]. Due to this mixing the lifetime of the $n = 1$ Landau level of the light holes is influenced by the lifetime of the heavy hole Landau levels. For streaming motion of the heavy holes the lifetime of the heavy holes is very short and therefore also the lifetime of $n = 1$ Landau level of the light holes is shorter than for higher Landau levels. This condition is necessary for the build up of a population inversion within the light hole sub-band.

To maintain streaming of heavy holes as the dominant pumping mechanism up to high magnetic fields the carrier drift has to be oriented in the direction of the highest mass. For the energy surface of light and heavy holes in the (110) plane (shown in the insert of Fig. 9) the constant energy lines for light holes are spherical, while they exhibit a warped contour for the heavy holes. The effective mass for heavy holes is largest in the $[\bar{1}\,1\,\bar{1}]$ direction. As a result the condition $\xi_h \leqslant 2$ will be maintained to higher magnetic fields for a given electric field. To direct the carrier drift into the $[\bar{1}\,1\,\bar{1}]$ direction a configuration $\mathbf{B} \| [110]$ and $\mathbf{E} \| [1\bar{1}0]$ has been chosen. The highest gain can be achieved when a sample geometry is used which takes into account that the total electric field – the sum of the applied Hall field ($\mathbf{E}_{tot} = [\mathbf{E}^2_{appl} + \mathbf{E}^2_{hall}]^{1/2}$), induces a streaming motion with the heaviest mass of $m^*_h = 0.44\, m_0$.

The gain of the cyclotron resonance laser is estimated to be $0.05 \pm 0.02\,cm^{-1}$. The gain can be calculated from the expression given by Wolff [3]:

$$g_e = \frac{e^2}{\varepsilon_0 c \eta m^*_e} n\,(f_n - f_{n-1})\,\frac{1}{\Delta\omega}$$

where η is the refractive index, $\Delta\omega$ the spontaneous linewidth, n the Landau level index and $|f_n - f_{n-1}|$ the population inversion. For $\Delta\omega = 3\,cm^{-1}$ and $n = 2$ a population inversion in the order of $5 \times 10^{10}\,cm^{-3}$ is necessary to explain the observed gain. This is a reasonable number considering the quite unselective pumping process by streaming motion.

In conclusion, we have observed strong stimulated CR emission from the light holes in germanium. The spectrum consists of a single line with a linewidth of about $0.2\,cm^{-1}$ and is linearly tunable between $65\,cm^{-1}$ and $85\,cm^{-1}$. With external mirrors the output power is increased and the fluctuations within the tuning range are reduced. We determine the gain to be $0.05 \pm 0.02\,cm^{-1}$ and identify the lasing transition to be the $n = 2$ to $n = 1$ Landau level transition of the light holes. The pumping mechanism is based on streaming motion of hot holes. A quantitative description taking into account the complete band structure and all relevant scattering processes has to be developed.

5. Using the cyclotron resonance laser for FIR spectroscopy

FIR spectroscopy has always been lacking of strong and tunable light sources. With the realization of tunable cyclotron resonance lasers in p-Ge the 'FIR gap' for wavelengths between 30 and 1000 μm is getting closed. Presently, cyclotron resonance lasers cover two wavelength ranges (Fig. 13): for a doping of $8 \times 10^{12}\,cm^{-3}$ a tuning range of 330 μm

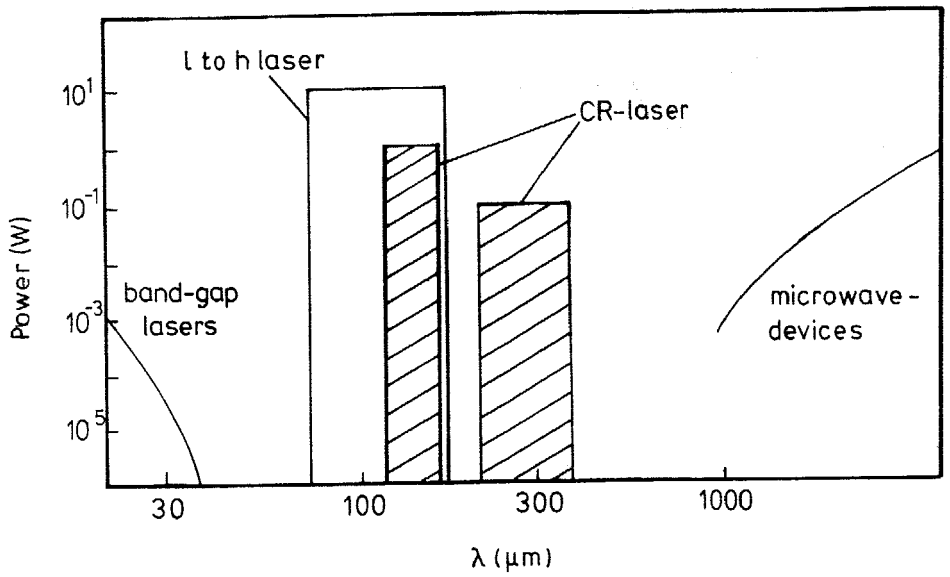

Figure 13 Intensities and frequencies of light to heavy hole (l to h) and cyclotron resonance (CR) *p*-Ge lasers.

(30 cm^{-1}) to 200 μm (50 cm^{-1}) is obtained; for a doping of 6×10^{13} cm^{-3} lasing is observed between 150 μm (65 cm^{-1}) and 110 μm (85 cm^{-1}). The emission power is considerably high (100 mW to 1 W). Due to the high power consumption and low operating temperature (T = 4.2 K) only pulsed operation and low duty cycles (0.5 to 1 μs, 10 Hz) are possible.

We have performed spectroscopy in GaAs/AlGaAs heterostructures using the cyclotron resonance (CR) laser as a FIR light source for the first time [47]. In Fig. 14 the transmission of the heterostructure is shown as a function of the magnetic field at the structure and for different frequencies of the CR laser: clear transmission minima can be observed due to cyclotron resonance absorption in the two dimensional electron gas of the heterostructure. The linewidth of the absorption is about 1.5 cm^{-1} and is in good agreement with the values obtained by a FIR gas laser [55]. These results demonstrate that the CR laser is a perfect tool for spectroscopy. A detailed study of the linewidth as a function of the filling factor is possible without changing the carrier concentration.

6. Summary

We have investigated the spectrum of the stimulated light–heavy hole emission of *p*-Ge using a narrowband tunable GaAs detector. The observed mode structure of samples without external resonators was quantitatively explained in terms of waveguide-like modes due to total reflections at the sample surfaces. By comparison with an external FIR gas laser the emission power was estimated to reach 500 mW. After attaching external mirrors laser operation on a single line was obtained. The possibility of step-wise tuning was demonstrated when the mode spacing of the external resonator is larger than the gain region.

Strong stimulated cyclotron resonance emission was observed from *p*-Ge samples with the magnetic field applied parallel to the [110] and the electric field parallel to the [1$\bar{1}$0] crystallographic directions. In this configuration the emission power is comparable to that of the stimulated light–heavy hole emission. Using different output couplers we have

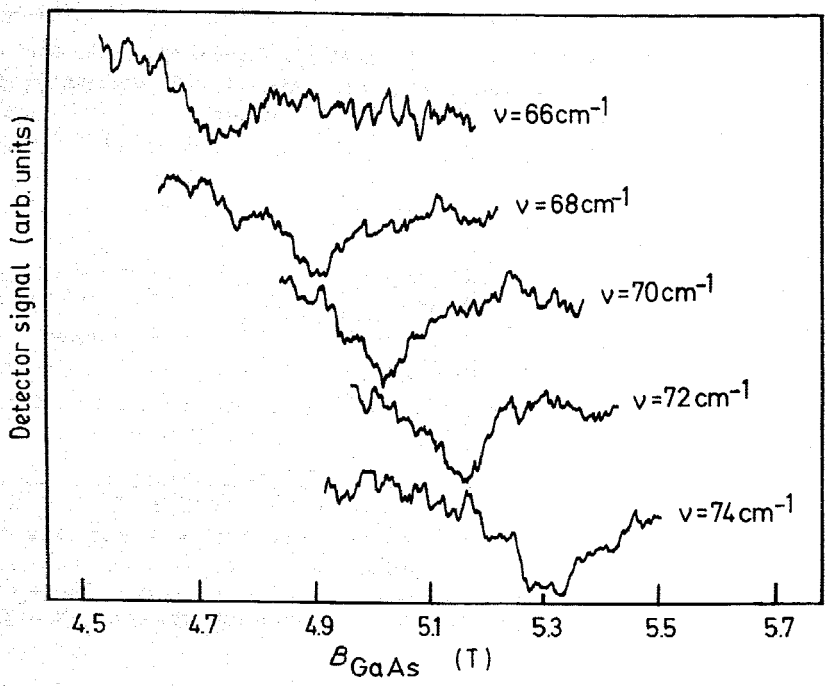

Figure 14 Transmission of a GaAs/AlGaAs heterostructure for different frequencies of the CR laser as a function of the magnetic field.

determined the gain to be $0.05 \pm 0.02\,cm^{-1}$. In order to help with the identification of the lasing transition we performed a cyclotron resonance absorption measurement with an external FIR gas laser and compared the results to the emission data. Using the Pidgeon and Brown model and second order perturbation theory for the influence of the electric field we identified the lasing transition to be the $n = 2$ to $n = 1$ Landau level transition of the light hole sub-band.

Through the realization of a tunable solid-state laser based on light hole cyclotron resonance transitions a quite remarkable breakthrough has been achieved in FIR spectroscopy. Using the CR laser we have performed measurements of the transmission and the photoconductive response of a GaAs/AlGaAs heterostructure as a function of the magnetic field. The considerable high emission power of the CR laser opens also the possibility of using these lasers in the large field of non-linear spectroscopy.

Acknowledgement

The work is partly supported by the Jubiläumsfonds der Österreichischen Nationalbank, Vienna, and Wild-Leitz, Heerbrugg, Switzerland.

References

1. H. KRÖMER, *Phys. Rev.* **109** (1958) 1856.
2. B. LAX, in 'Quantum Electronics', (Columbia University Press, New York, 1960) p. 428.
3. P. A. WOLFF, *Physics* **1** (1964) 147.
4. E. GORNIK, *Phys. Rev. Lett.* **29** (1972) 595.
5. E. OTSUKA, K. L. KOBAYASHI and K. F. KOMATSUBARA, *Phys. Rev. Lett.* **30** (1973) 702.

6. YU. L. IVANOV and YU. V. VASIL'EV, *Sov. Tech. Phys. Lett.* **9**(1983) 264.
7. A. A. ANDRONOV, I. V. ZVEREV, V. A. KOZLOV, YU. N. NOZDRIN, S. A. PAVLOV and V. N. SHASTIN, *Sov. Phys. JETP Lett.* **40** (1984) 804.
8. T. KUROSAWA, *J. Phys. Soc. Jpn* **21** (1966) Suppl. 424.
9. I. I. VOSILYUS and I. B. LEVINSON, *Sov. Phys. JETP* **25** (1967) 672.
10. I. I. VOSILYUS, *Sov. Phys. Solid State* **11** (1969) 755.
11. T. KUROSAWA and H. MAEDA, *J. Phys. Soc. Jpn* **31** (1971) 668.
12. H. MAEDA and T. KUROSAWA, Proceedings of the 11th International Conference on the Physics of Semiconductors (Warsaw 1972), p. 602.
13. YA. I. AL'BER, A. A. ANDRONOV, V. A. VALOV, V. A. KOZLOV, A. M. LERNER and I. P. RYAZANTSEVA, *Sov. Phys. JETP* **45** (1977) 539.
14. T. KUROSAWA, *Solid State Commun.* **24** (1977) 357.
15. A. A. ANDRONOV, V. A. KOZLOV, L. S. MAZOV and V. N. SHASTIN, *Sov. Phys. JETP Lett.* **30** (1979) 551.
16. T. KUROSAWA, *J. Physique* **42** (1981) Supplement 10 C7–377.
17. A. A. ANDRONOV, E. P. DODIN and Z. F. KRASIL'NIK, *Sov. Phys. Semicond.* **16** (1982) 133.
18. A. A. ANDRONOV and YU. K. POZHELA, in 'Hot electrons in semiconductors: streaming and anisotropic distributions in crossed fields and inverted distributions of hot electrons in semiconductors', (in Russian) edited by Andronov and Pozhela, (Gorky 1983).
19. S. KOMIYAMA, T. KUROSAWA and T. MASUMI, in 'Topics in Applied Physics', Hot Electron Transport in Semiconductors, Vol. 58, edited by Regiani (Springer–Verlag, Berlin, 1985) p. 177.
20. A. A. ANDRONOV *et al.*, *Physica* **134B** (1985) 210.
21. YU. A. MITYAGIN, V. N. MURZIN, S. A. STOKLITSKII and I. E. TROFIMOV, *Sov. Phys. JETP Lett.* **46** (1987) 144.
22. A. A. ANDRONOV, YU. N. NOZDRIN and V. N. SHASTIN, *Infrared Phys.* **27** (1987) 31.
23. YU. K. POZHELA, E. V. STARIKOV and P. N. SHIKTOROV, *Sov. Phys. Semicond.* **17** (1983) 566.
24. *Idem. Phys. Lett.* **96A** (1983) 361.
25. Y. I. AL'BER, A. A. ANDRONOV, V. A. VALOV, V. A. KOZLOV and I. R. RYAZANTSEVA, *Solid State Commun.* **19** (1976) 955.
26. M. HELM and E. GORNIK, *Phys. Rev.* **B34** (1986) 7459.
27. M. HELM, K. UNTERRAINER and E. GORNIK, *Phys. Rev.* **B39** (1989) 6212.
28. A. KOZLOV, L. S. MAZOW, I. M. NEFEDOV and M. R. ZABOLOTSKIKH, *Sov. Phys. JETP Lett.* **37** (1983) 170.
29. M. I. D'YAKONOV and V. I. PEREL', *Sov. Phys. JETP* **65**, (1987) 200.
30. B. M. GORBOVITSKII, *Sov. Phys. Semicond.* **18** (1984) 437.
31. YU. L. IVANOV, *Sov. Phys. JETP Lett.* **34** (1981) 515.
32. S. KOMIYAMA, *Phys. Rev. Lett.* **48** (1982) 271.
33. V. I. GAVRILENKO, V. N. MURZIN, S. A. STOKLITSKII and V. P. CHEBOTAREV, *Sov. Phys. JETP Lett.* **35** (1982) 97.
34. A. A. ANDRONOV, V. I. GAVRILENKO, O. F. GRISHIN, V. N. MURZIN, YU. N. NOZDRIN, S. A. STOKLITSKII, A. P. CHEBOTAREV and V. N. SHASTIN, *Sov. Phys. Dokl.* **27** (1982) 932.
35. S. KOMIYAMA, N. IIZUKA and Y. AKASAKA, *Appl. Phys. Lett.* **47** (1985) 958.
36. M. HELM, K. UNTERRAINER, E. GORNIK and E. E. HALLER, *Solid State Electron.* **31** (1988) 759.
37. S. KOMIYAMA, *Adv. Phys.* **31** (1982) 255.
38. E. GORNIK, *Physica* **127B** (1984) 95.
39. S. KOMIYAMA and S. KURODA, *Solid State Commun.* **59** (1986) 167.
40. S. KOMIYAMA, Proceedings of the 18th International Conference on the Physics of Semiconductors. (World Scientific, Singapore 1987) p. 1641.
41. A. ANDRONOV, A. MURAVJEV, I. NEFEDOV, Y. NOZDRIN, S. PAVLOV, V. SHASTIN, Y. MITYAGIN, V. MURZIN, S. A. STOKLITSKII, I. TROFIMOV and A. CHEBOTAREV, Proceedings of the 18th International Conference on the Physics of Semiconductors (World Scientific, Singapore 1987) p. 1663.
42. K. UNTERRAINER, M. HELM, E. GORNIK, E. E. HALLER and J. LEOTIN, *Appl. Phys. Lett.* **52** (1988) 564.
43. K. UNTERRAINER, M. NITHISOONTORN, M. HELM, E. GORNIK and E. E. HALLER, *Infrared Physics* **29** (1989) 357.
44. YU. B. VASIL'EV and YU. L. IVANOV, *Sov. Tech. Phys. Lett.* **10** (1984) 398.
45. *Idem.* Proceedings of the 18th International Conference on the Physics of Semiconductors (World Scientific, Singapore, 1987) p. 1659.

46. Y. A. MITYAGIN, V. N. MURZIN, S. A. STOKLITSKIJ, I. E. TROFIMOV and A. P. CHEBOTAREV, Proceedings 19th International Conference on the Physics of Semiconductors (Warsaw, 1988) p. 1439.
47. K. UNTERRAINER, C. KREMSER, E. GORNIK and YU. L. IVANOV, *Solid State Electron* **32** (1989) 1527.
48. K. UNTERRAINER, C. KREMSER, E. GORNIK, C. R. PIDGEON, YU. L. IVANOV and E. E. HALLER, *Phys. Rev. Lett.* **64** (1990) 2277.
49. J. M. LUTTINGER, *Phys. Rev.* **102** (1956) 1030.
50. K. SUZUKI and J. C. HENSEL, *Phys. Rev.* B **9** (1974) 4184.
51. J. C. HENSEL and M. PETER, *Phys. Rev.* **114** (1959) 411.
52. C. R. PIDGEON and R. N. BROWN, *ibid.*, **146** (1966) 575.
53. Q. H. F. VREHEN, *ibid.*, **145** (1966) 675.
54. Q. H. F. VREHEN, *Phys. Rev. Lett.* **14** (1965) 558.
55. W. SEIDENBUSCH, E. GORNIK and G. WEIMANN, *Phys. Rev.* **B36** (1987) 9155.